Intercellular adhesion molecule-1 is a regulator of blood–testis barrier function

Xiang Xiao, C. Yan Cheng and Dolores D. Mruk*

Center for Biomedical Research, Population Council, 1230 York Avenue, New York, NY 10065, USA

*Author for correspondence (mruk@popcbr.rockefeller.edu).

Accepted 12 August 2012
Journal of Cell Science 125, 5677–5689

doi: 10.1242/jcs.107987

Summary

The mechanism underlying the movement of preleptotene/leptotene spermatocytes across the blood–testis barrier (BTB) during spermatogenesis is not well understood largely owing to the fact that the BTB, unlike most other blood–tissue barriers, is composed of several co-existing and co-functioning junction types. In the present study, we show that intercellular adhesion molecule-1 [ICAM-1, a Sertoli and germ cell adhesion protein having five immunoglobulin (Ig)-like domains, in addition to transmembrane and cytoplasmic domains] is a regulator of BTB integrity. Initial experiments showed ICAM-1 to co-immunoprecipitate and co-localize with tight junction and basal ectoplasmic specialization proteins such as occludin and N-cadherin, which contribute to BTB function. More importantly, overexpression of ICAM-1 in Sertoli cells *in vitro* enhanced barrier function when monitored by transepithelial electrical resistance measurements, illustrating that ICAM-1-mediated adhesion can promote BTB integrity. On the other hand, overexpression of a truncated form of ICAM-1 that consisted only of the five Ig-like domains (*s*ICAM-1; this form of ICAM-1 is known to be secreted) elicited an opposite effect when Sertoli cell barrier function was found to be perturbed *in vitro*; in this case, *s*ICAM-1 overexpression resulted in the downregulation of several BTB constituent proteins, which was probably mediated by Pyk2/p-Pyk2-Y402 and c-Src/p-Src-Y530. These findings were expanded to the *in vivo* level when BTB function was found to be disrupted following *s*ICAM-1 overexpression. These data illustrate the existence of a unique mechanism in the mammalian testis where ICAM-1 can either positively or negatively regulate BTB function.

Key words: Intercellular adhesion molecule-1, Tight junction, Blood–testis barrier, Sertoli cell, Testis

Introduction

Throughout spermatogenesis, many critical biochemical, cellular and morphological events take place. These events allow germ cells to traverse the seminiferous epithelium while developing into elongated spermatids that are eventually released into the tubule lumen at late stage VIII of the seminiferous epithelial cycle during spermiation (Cheng and Mruk, 2002; de Kretser and Kerr, 1988; Mruk and Cheng, 2004; O'Donnell et al., 2011). For example, many different junction types are known to constitute the function of the blood–testis barrier (BTB, also known as the Sertoli cell barrier). These include tight junctions (TJs), basal ectoplasmic specializations (ES), gap junctions (GJs) and desmosomes, and they must disassemble intermittently during stages VIII–XI to allow zygotene spermatocytes to enter the adluminal compartment without compromising the homeostasis of the seminiferous epithelium and without affecting spermatogenesis (Cheng and Mruk, 2012; Mruk and Cheng, 2004). To achieve this, the testis has a unique mechanism in place where preleptotene/leptotene spermatocytes are briefly trapped within an intermediate compartment that is sealed at north and south poles by TJs, basal ESs, GJs and desmosomes (Mruk and Cheng, 2008; Russell, 1993a; Yan et al., 2008). The only way that spermatocytes can move upwards in the seminiferous epithelium is if these junctions, which are situated immediately in front of spermatocytes, are disassembled. Before this can occur, though, Sertoli cells must assemble a functional BTB behind spermatocytes, illustrating that an enormous amount of coordinated restructuring is taking place at the BTB (Cheng and Mruk, 2009; Cheng and Mruk, 2012). Unfortunately, the mechanism of junction assembly and disassembly at the BTB still remains incompletely understood.

In this report, we show for the first time that intercellular adhesion molecule-1 (ICAM-1) is a critical regulator of BTB dynamics. ICAMs are immunoglobulin (Ig)-like adhesion proteins residing largely on the cell surface, and five members (ICAM-1, -2, -3, -4 and -5) have been identified to date (Lawson and Wolf, 2009; Long, 2011; Muller, 2011). Of these, ICAM-1 is the best studied with respect to the movement of leukocytes across the endothelium during infection and inflammation where it is known to 'seal' the endothelium as migrating leukocytes cross it (somewhat analogous to the intermediate compartment in the testis), thereby maintaining barrier integrity (Dustin et al., 1986; Mamdouh et al., 2009; Nourshargh et al., 2010; Rothlein et al., 1986). A soluble form of ICAM-1 (*s*ICAM-1), which is comprised of the entire or a portion of the extracellular domain of ICAM-1 and most likely derived from proteolytic cleavage of membrane-bound ICAM-1, has also been described to have important biological functions in other epithelia (Gearing et al., 1992; Lawson and Wolf, 2009; Marlin et al., 1990; Rothlein et al., 1991; van de Stolpe and van der Saag, 1996; Witkowska and Borawska, 2004). Herein, we show that Sertoli cell surface-associated ICAM-1 enhanced BTB function by facilitating cross-talk among different junction types, illustrating that ICAM-1 is working below spermatocytes to strengthen barrier function during stages VIII-XI of the seminiferous epithelial cycle. On the

Journal of Cell Science

other hand, *s*ICAM-1 was found to be a negative regulator of Sertoli cell barrier/BTB function, demonstrating that junction disassembly above migrating spermatocytes is facilitated in part by ICAM-1 cleavage.

Results

ICAM-1 localizes to the BTB stage-specifically in the adult rat testis

A survey of different ICAM family members in selected rat organs was performed using RT–PCR (supplementary material Fig. S1; Table S1). Of these, *Icam-1* and *Icam-2* were expressed by the testis (supplementary material Fig. S1Aa,B), whereas *Icam-4* and *Icam-5* were restricted to the liver and brain, respectively (supplementary material Fig. S1C,D). *Icam-1* RT–PCR results were verified by immunoblotting (supplementary material Fig. S1Ab). ICAM-1 was then localized in the adult rat testis by using a rabbit polyclonal antibody targeting the cytoplasmic domain of rat ICAM-1 (supplementary material Table S2) for immunohistochemistry (Fig. 1A). It should be noted that this antibody was found to cross-react with full-length (membrane-associated) ICAM-1 (97 kDa, referred to as ICAM-1 in this study), but it did not noticeably cross-react with soluble (extracellular) ICAM-1 (~70 kDa). ICAM-1 immunoreactivity associated with Sertoli and germ cells at all stages of the seminiferous epithelial cycle (Fig. 1Ab–h). Discrete ICAM-1 staining was found to surround the heads of elongating and elongated spermatids at stages IX–XIII (Fig. 1Af–h). Moreover, ICAM-1 immunoreactivity was stage-specific at the site of the BTB (highest at stage VIII; Fig. 1Ab,d,e). No staining was observed when anti-ICAM-1 IgG was replaced with rabbit IgG (Fig. 1Aa). By immunoblotting, the monospecificity of the ICAM-1 antibody was assessed (Fig. 1B). A protein band corresponding to ICAM-1 was seen in lysates from Sertoli and germ cells, as well as in the testis, and these data were in agreement with RT–PCR results (Fig. 1C), as well as with previous reports from other laboratories (De Cesaris et al., 1998; Riccioli et al., 1995).

ICAM-1 is an integral component of the BTB

To expand the above findings, co-immunoprecipitation (co-IP) was performed to identify protein–protein interactions at the BTB (Fig. 2A). ICAM-1 structurally interacted with occludin (but not with claudin-11 or coxsackie and adenovirus receptor [CAR]), zonula occludens-1 (ZO-1), N-cadherin and β-catenin, as well as with actin, a cytoskeleton protein (Fig. 2A). It is worth noting that previous studies have shown all of these proteins to localize to the Sertoli cell barrier/BTB (Cheng and Mruk, 2012; Cyr et al., 1999; Hellani et al., 2000; Mruk and Cheng, 2004; Su et al., 2010a; Wang et al., 2007; Wong et al., 2004). To validate that ICAM-1 was indeed a constituent protein of the BTB, Sertoli cells (previously cultured for 4 days and having a functional barrier that mimicked the BTB *in vivo*) were fluorescently immunostained and analyzed by confocal microscopy (Fig. 2B). ICAM-1 was found to partially co-localize with occludin and N-cadherin at the Sertoli cell barrier when corresponding images were merged (Fig. 2Ba–h). This is in agreement with previous reports that used other models (Millán et al., 2006; Yang et al., 2005), as well as with subsequent experiments that used adult testes for immunofluorescent staining. Here, ICAM-1 partially co-localized with occludin and ZO-1, as well as with N-cadherin and β-catenin at the BTB (Fig. 2Ca–p). ICAM-1 immunoreactivity was most intense at the site of the BTB at stage VIII of the seminiferous epithelial cycle (Fig. 2Cb–d,f–h,j–l,n–p), consistent with immunohistochemistry results (Fig. 1A).

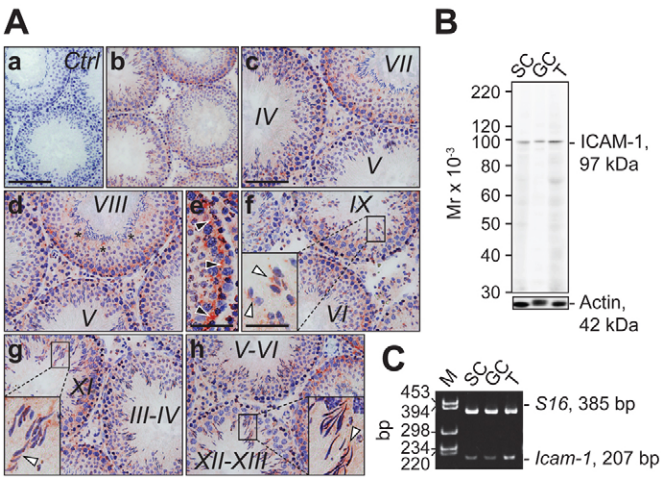

Fig. 1. Presence of ICAM-1 in Sertoli cells, germ cells and adult rat testes shown by immunohistochemistry, immunoblotting and RT-PCR. (**A**) Frozen testes from control rats were cut at 7 μm, and immunohistochemistry was performed using a rabbit polyclonal antibody targeting the cytoplasmic domain of rat ICAM-1 (supplementary material Table S2). ICAM-1 immunoreactivity, which appeared as reddish-brown precipitates [3-amino-9-ethylcarbazole (AEC), b–h], was stage-specific. Stages of the seminiferous epithelial cycle are denoted as roman numerals (c,d,f–h). For the control (Ctrl), anti-ICAM-1 IgG was replaced with rabbit IgG, which was used at the same dilution (a). Asterisks (d) denote the luminal edge of a stage VIII tubule and show the presence of ICAM-1 before spermiation. Black arrowheads (e) point to the site of the BTB in a stage VIII tubule where ICAM-1 immunoreactivity was highest. Boxed areas (f–h) correspond to magnified images, which better depict ICAM-1 staining at the apical ES (white arrowheads). Scale bar in a (also applies to b)=200 μm; scale bar in c (also applies to d,f–h)=140 μm; scale bar in e=70 μm; and scale bar in inset in f (also applies to insets in g,h)=45 μm. (**B**) Sertoli cell (SC, cultured for 5 days *in vitro*), germ cell (GC, freshly isolated) and testis (T) lysates (~50 μg protein/lane) were used for immunoblotting to demonstrate the monospecificity of the ICAM-1 antibody prior to its use for immunohistochemistry, as well as to show the presence of ICAM-1 in these cells and in this organ. The relative positions of protein bands corresponding to the MagicMark™ XP Western Protein Standard (Invitrogen) are noted to the left. Actin served as an internal control. Mr, molecular mass. (**C**) RT–PCR results for *Icam1* using RNAs from Sertoli cells, germ cells and testis. *S16* was used as an internal control. bp, base pairs; M, DNA molecular mass marker VI (Roche).

*s*ICAM-1 is present in Sertoli and germ cells

Recombinant *s*ICAM-1 embodying rat extracellular ICAM-1 domains 2 and 3 was produced by *Escherichia coli* (supplementary material Table S1), and protein lysates obtained from soluble and insoluble fractions from both uninduced and induced bacterial cell cultures were resolved by SDS-PAGE. A predominant protein of 24 kDa was noted by Coomassie blue gel staining (Fig. 3A). Production of His_6-tagged recombinant *s*ICAM-1 was verified first by a His_6 antibody (Fig. 3B) and second by a commercially available ICAM-1 antibody (data not shown) (supplementary material Table S2). This commercially available antibody, raised against the extracellular domain of rat ICAM-1, was predicted to cross-react with *s*ICAM-1. Indeed, a protein of 24 kDa, corresponding to recombinant *s*ICAM-1, was

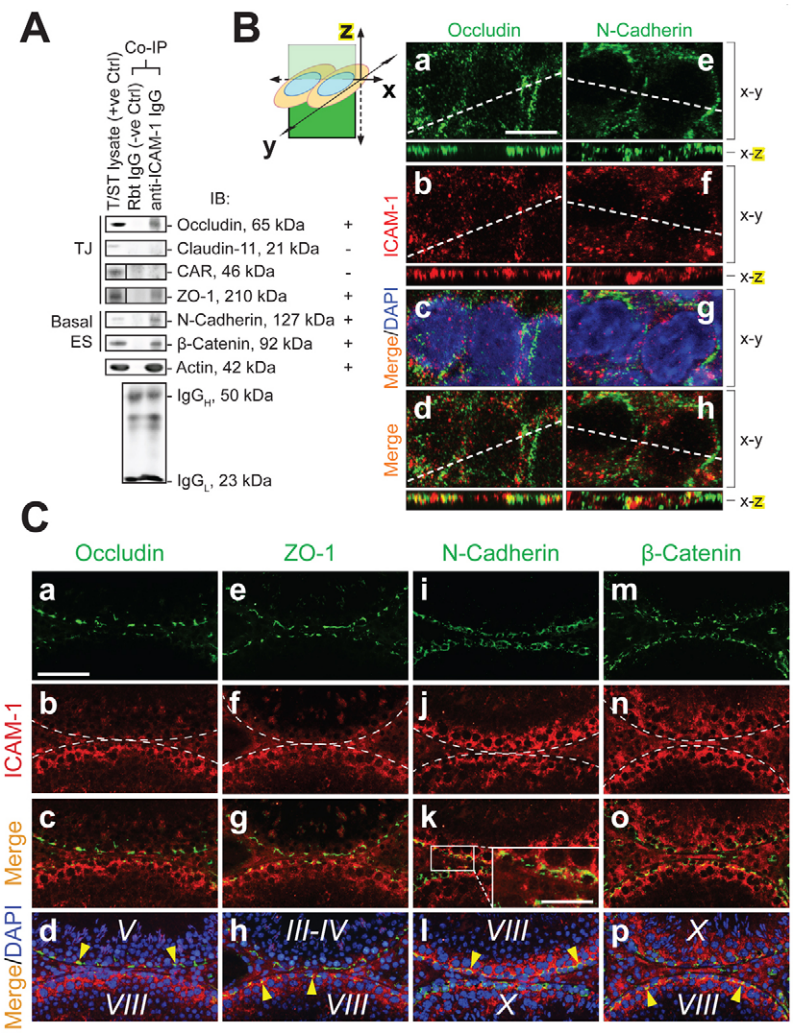

Fig. 2. ICAM-1 is an integrated component of the BTB as demonstrated by co-IP experiments, confocal microscopy and dual-labelled immunofluorescent staining. (**A**) Co-IP experiments to determine the structural interactions between ICAM-1 and selected BTB constituent proteins when testis (T) or seminiferous tubule (ST) lysates (~600–800 µg protein/sample) were used. For the positive control (+ve Ctrl), T or ST lysates (~20–50 µg protein/lane) were used without co-IP. For the negative control (-ve Ctrl), anti-ICAM-1 IgG was replaced with rabbit (Rbt) IgG (supplementary material Table S2). IgG_H and IgG_L represent IgG heavy and light chains, respectively. This representative immunoblot also shows the uniform processing of samples. +, positive co-IP result; -, negative co-IP result. Proteins are categorized as TJ or basal ES proteins to the left of immunoblots. (**B**) To examine the co-localization of ICAM-1 with TJ and basal ES proteins in Sertoli cells, confocal microscopy was performed by using anti-ICAM-1 IgG (red, b,f) in conjunction with anti-occludin (green, a) or anti-N-cadherin IgG (green, e) (supplementary material Table S2). Cell nuclei were stained with DAPI (blue, c,g). Corresponding images were merged (c,d,g,h). As shown in the illustration to the left, images are presented as x-y and x-z planes, and the z-plane (yellow highlight) represents the plane at which partial co-localization of proteins at the Sertoli cell barrier is noted. Dashed straight lines (a,b,d–f,h) mark the sites at which x-z images were obtained, and these are shown immediately below x-y images. Scale bar in a (also applies to b–h)=15 µm. (**C**) To examine the co-localization of ICAM-1 with TJ and basal ES proteins in the testis, dual-labeled immunofluorescent staining was performed by using anti-ICAM-1 IgG (red, b,f,j,n) in conjunction with anti-occludin (a), anti-ZO-1 (e), anti-N-cadherin (i) or anti-β-catenin (m) IgG (green) (supplementary material Table S2). Cell nuclei were stained with DAPI (d,h,l,p). Corresponding images were merged (c,d,g,h,k,l,o,p). Yellow arrowheads (d,h,l,p) point to the partial co-localization of ICAM-1 with BTB constituent proteins. Stages of the seminiferous epithelial cycle are denoted as roman numerals (d,h,l,p). The boxed area in (k) corresponds to the magnified image (inset), which better depicts the partial co-localization of ICAM-1 with N-cadherin. Dashed curved lines (b,f,j,n) mark the periphery of seminiferous tubules. Scale bar in a (also applies to b–p)=100 µm; scale bar in inset in k=40 µm.

noted in agreement with experiments that used the His_6 antibody (data not shown). However, this antibody was not used for any of the other experiments reported in this study because its use yielded results of poor quality. When testis, Sertoli cell (cultured for 5 days *in vitro*) and germ cell (freshly isolated) lysates were used for immunoblotting in conjunction with the *s*ICAM-1 antibody produced by us (supplementary material Table S2), a ~70 kDa protein was observed in all samples (Fig. 3C). A 97 kDa protein corresponding to membrane-associated ICAM-1 (see Fig. 1B) was also weakly detected in all samples with the *s*ICAM-1 antibody. It is worth noting that ICAM-1 and *s*ICAM-1 levels were consistently lowest in Sertoli cells. Finally, proteins of lower M_r were also noted, and they may represent other *s*ICAM-1 fragments, which may or may not exert biological activity in the testis. At this point, additional experiments would be needed to support this postulate (Fig. 3C).

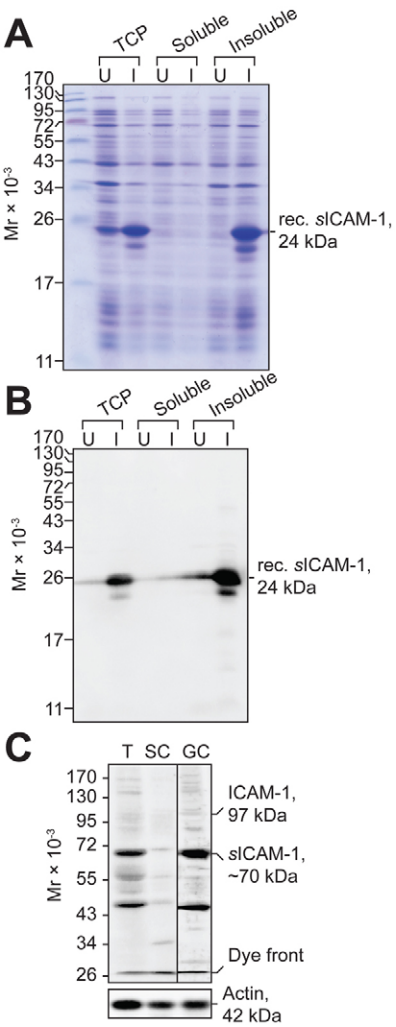

Fig. 3. Production of a polyclonal *s*ICAM-1 antibody and the presence of *s*ICAM-1 in the testis. (**A**) Recombinant *s*ICAM-1 (rec. *s*ICAM-1) was expressed in *E. coli*, protein lysates obtained from soluble and insoluble fractions from both uninduced (U) and induced (I) bacterial cell cultures (~100 μg protein/lane) were resolved by SDS-PAGE, and the gel was stained with Coomassie Blue. TCP, total cell protein. (**B**) Protein lysates (~50 μg protein/lane) obtained from the above experimental step and identical to those shown in A were used for immunoblotting. Production of His_6-tagged rec. *s*ICAM-1 was verified first by a His_6 antibody (B) and secondly by an ICAM-1 antibody (data not shown; it should be noted that this commercially available ICAM-1 antibody was raised against the extracellular domain of rat ICAM-1) (supplementary material Table S2). (**C**) Testis, Sertoli cell (SC, cultured for 5 days *in vitro*) and germ cell (GC, freshly isolated) lysates (~30 μg protein/lane) were used for immunoblotting to demonstrate the monospecificity of the *s*ICAM-1 antibody, as well as to show the presence of *s*ICAM-1 in this organ and in these cells. Actin served as an internal control. The relative positions of protein bands corresponding to the MagicMark™ XP Western Protein Standard (Invitrogen) are noted to the left (A–C). Mr, molecular mass.

Opposed effects of ICAM-1 and *s*ICAM-1 overexpression on Sertoli cell barrier function *in vitro*

When DNA constructs embodying either full-length ICAM-1 or *s*ICAM-1 lacking transmembrane and cytoplasmic domains (Fig. 4A) were transfected into Sertoli cells at time 0, an increase in the *Icam-1* mRNA level was detected by semi-quantitative (supplementary material Fig. S2Aa,b) and quantitative (supplementary material Fig. S2Ba,b) PCR when compared with Sertoli cells that were transfected with the pCI-neo/MOCK (control) plasmid. Co-IP and immunoblotting were also used to verify PCR results and to assess changes following ICAM-1 (Fig. 4Ba,b) and *s*ICAM-1 (Fig. 4Ca,b) overexpression. Two days after ICAM-1 transfection, a significant increase in transepithelial electrical resistance (TER) was detected, which was maintained until the next day (Fig. 4Bc). By contrast, *s*ICAM-1 overexpression resulted in a decline in TER, demonstrating a disruption of Sertoli cell barrier function (Fig. 4Cc). Specificity was addressed by overexpression of another ICAM family member, namely ICAM-2 (supplementary material Fig. S3). By immunofluorescent staining, ICAM-2 was found to localize to spermatocytes and elongated spermatids (supplementary material Fig. S3Aa,b). Interestingly, ICAM-2 did not co-localize with ZO-1 (supplementary material Fig. S3Aa,b), illustrating that ICAM-2 is not a constituent protein of the BTB. Following ICAM-2 overexpression, an increase in the ICAM-2 protein level was noted when compared with the corresponding control, illustrating successful overexpression *in vitro* (supplementary material Fig. S3B,a,b). As expected, ICAM-2 overexpression did not affect the integrity of the Sertoli cell barrier when its function was assessed by TER (supplementary material Fig. S3C). These results illustrate that the changes that we observed following ICAM-1 and *s*ICAM-1 overexpression were specific to ICAM-1 and *s*ICAM-1. Finally, it is worth noting that Sertoli cell viability was not significantly affected by Effectene® transfection reagent because TER readings did not decrease following transfection of pCI-neo/MOCK-containing plasmids (Fig. 4Bc,Cc).

*s*ICAM-1 overexpression *in vitro* down-regulates integral membrane proteins and adaptors at the Sertoli cell barrier via c-Src and Pyk2-dependent pathways

To further investigate the disruptive effects of *s*ICAM-1 overexpression on Sertoli cell barrier function, we investigated the steady-state levels of different integral membrane, scaffolding and regulatory proteins known to be present at the BTB (Fig. 5A,B). Immunoblotting revealed no changes in the steady-state levels of occludin, ZO-1, CAR, junctional adhesion molecule-A (JAM-A), claudin-11, α-catenin, β-catenin, desmocollin-3, p130Cas and focal adhesion kinase (FAK)/p-FAK-Y397/p-FAK-Y407 following *s*ICAM-1 overexpression (Fig. 5A,B). However, *s*ICAM-1 overexpression brought about a decrease in the levels of N-cadherin and γ-catenin, as well as in levels of the GJ protein connexin 43 and two tyrosine kinases, proline-rich tyrosine kinase 2 (Pyk2)/p-Pyk2-Y402 and c-Src/p-Src-Y530 (Fig. 5A,B). Thereafter, these findings were validated by immunofluorescent staining. While no changes were observed in JAM-A, claudin-11, CAR and ZO-1 localization (Fig. 5C), a loss in N-cadherin, γ-catenin and connexin 43 from the Sertoli-Sertoli cell interface was noted following *s*ICAM-1 overexpression (Fig. 5C). These changes are in agreement with immunoblotting results (Fig. 5A,B). Finally, ultrastructural analysis by electron microscopy was performed on Sertoli cells 2 days after transfection with pCI-neo/MOCK- or *s*ICAM-1-containing plasmids (Fig. 5D). Following pCI-neo/MOCK overexpression, the integrity of the Sertoli cell barrier was maintained. On the other hand, several breaks were observed at sites of cell–cell contact following *s*ICAM-1 overexpression, illustrating that the integrity of Sertoli cell barrier was disrupted (Fig. 5D).

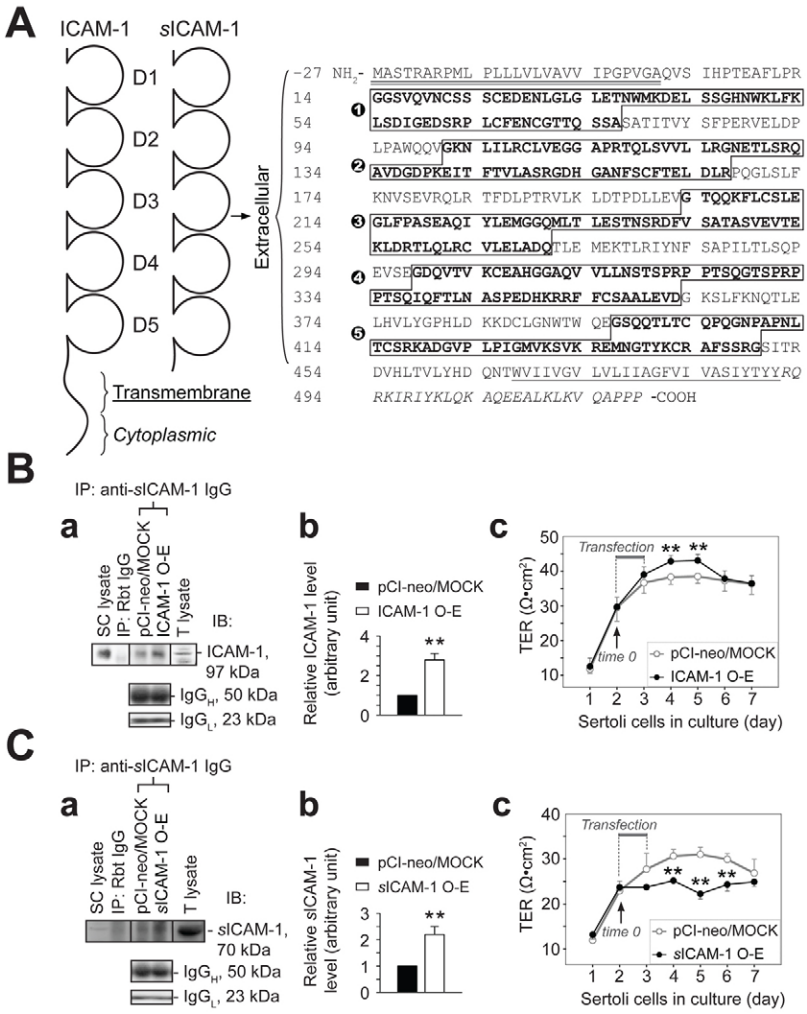

Fig. 4. Preparation of ICAM-1 and *s*ICAM-1 constructs based on the primary amino acid sequence of rat ICAM-1 and their effects on Sertoli cell barrier function after transient overexpression *in vitro*. (**A**) Schematic drawing of ICAM-1 (left) and *s*ICAM-1 (right). ICAM-1 contains five Ig-like domains (D1–D5), a transmembrane domain and a cytoplasmic domain. Primary amino acid sequence corresponding to rat ICAM-1 (far right). The five Ig-like domains are denoted in bold, boxed and numbered. The putative signal peptide is double-underlined. The transmembrane domain is underlined, and the cytoplasmic domain is in italics. (**B**,**C**) Sertoli cells were cultured for 2 days to establish a functional barrier. They were then transfected with pCI-neo/MOCK, ICAM-1 or sICAM-1 containing plasmids (this time point was designated as time 0). Sertoli cells were terminated 2 days after transfection for lysate preparation, and co-IP experiments were performed (Ba,Ca). For the positive controls, Sertoli cell (SC, ~60 μg protein/sample) and testis (T, ~100 μg protein/sample) lysates were used without co-IP (Ba,Ca). For the negative control, anti-*s*ICAM-1 (Ba,Ca) IgG was replaced with rabbit (Rbt) IgG (supplementary material Table S2). IgG_H and IgG_L represent IgG heavy and light chains, respectively. These representative immunoblots also show the uniform processing of samples. IP, immunoprecipitation; IB, immunoblotting. (Bb,Cb) Histograms summarizing co-IP/immunoblotting results. ICAM-1 and *s*ICAM-1 overexpression data points were normalized against their corresponding pCI-neo/MOCK overexpression data points, which were arbitrarily set at 1. Each data point is a mean±s.d. of at least three independent co-IP experiments (**$P<0.01$). TER was monitored daily in functional experiments (Bc,Cc). ICAM-1 overexpression increased TER and promoted Sertoli cell barrier integrity (Bc), whereas *s*ICAM-1 overexpression disrupted Sertoli cell barrier function (Cc). Each data point is a mean±S.D. of quintuplicate Millicell inserts within a representative experiment, and this experiment was repeated three times using different batches of Sertoli cells (**$P<0.01$). O-E, overexpression.

*s*ICAM-1 overexpression affects spermatogenesis and germ cell adhesion

We next investigated the physiological role of *s*ICAM-1 at the BTB by assessing barrier integrity following *s*ICAM-1 overexpression *in vivo*. An increase in *Icam-1* mRNA and protein levels was detected following *s*ICAM-1 overexpression by semi-quantitative (Fig. 6A) and real-time (Fig. 6B) PCR, as well as by co-IP and immunoblotting (Fig. 6C,D) when compared with testes that were transfected with the pCI-neo/MOCK plasmid, illustrating successful overexpression *in vivo*. Following *s*ICAM-1 overexpression, drastic morphological changes were observed 2–3 days after the last administration of DNA (Fig. 6E). These changes included the loss of spermatocytes and round spermatids from the seminiferous epithelium, and an increase in seminiferous tubule diameter (Fig. 6E). Also, elongated spermatids were mis-oriented within the epithelium (Fig. 6F). It is worth noting that obvious morphological changes in testes were noted in ~30% of animals when cross-sections were examined microscopically. From these animals, cross-sections were obtained from the center of testes (near injection sites), and within each cross-section, ~30% of tubules showed damage. No changes were observed after the administration of pCI-neo/MOCK-containing plasmids (Fig. 6E,F). A shortening of the seminiferous epithelium (in terms of height) was also observed (Fig. 6E–G). While an increase in seminiferous tubule diameter was observed following sICAM-1 overexpression (Fig. 6E,F), there was no significant increase in testis weight because this was offset by germ cell loss (data not shown). The reason for this increase in seminiferous tubule diameter is not immediately known. Magnified images from this experiment are also shown in supplementary material Fig. S4.

*s*ICAM-1 overexpression disrupts BTB integrity *in vivo*

Finally, BTB function was assessed following *s*ICAM-1 overexpression *in vivo*. For the positive control ($CdCl_2$), inulin-fluorescein isothiocyanate (FITC) was found to penetrate the BTB and to enter the adluminal compartment of the seminiferous epithelium (Fig. 6Ha,b), illustrating BTB disruption. This is in line with previously published reports, which showed $CdCl_2$ to disrupt BTB integrity (Durieu-Trautmann et al., 1994; Elkin et al., 2010; Prozialeck et al., 2006; Siu et al., 2009; Wong et al., 2004). For the negative control (pCI-neo/MOCK), inulin-FITC was restricted to the basal compartment (Fig. 6Hc,d). When *s*ICAM-1 constructs were transfected into testicular cells, inulin-FITC was found to enter the adluminal compartment 2 days after the last administration of DNA (Fig. 6He,f). Images were analyzed by measuring the distance traveled by inulin-FITC (D_{FITC}) and by measuring the radius of the seminiferous tubule (Dr). Data are

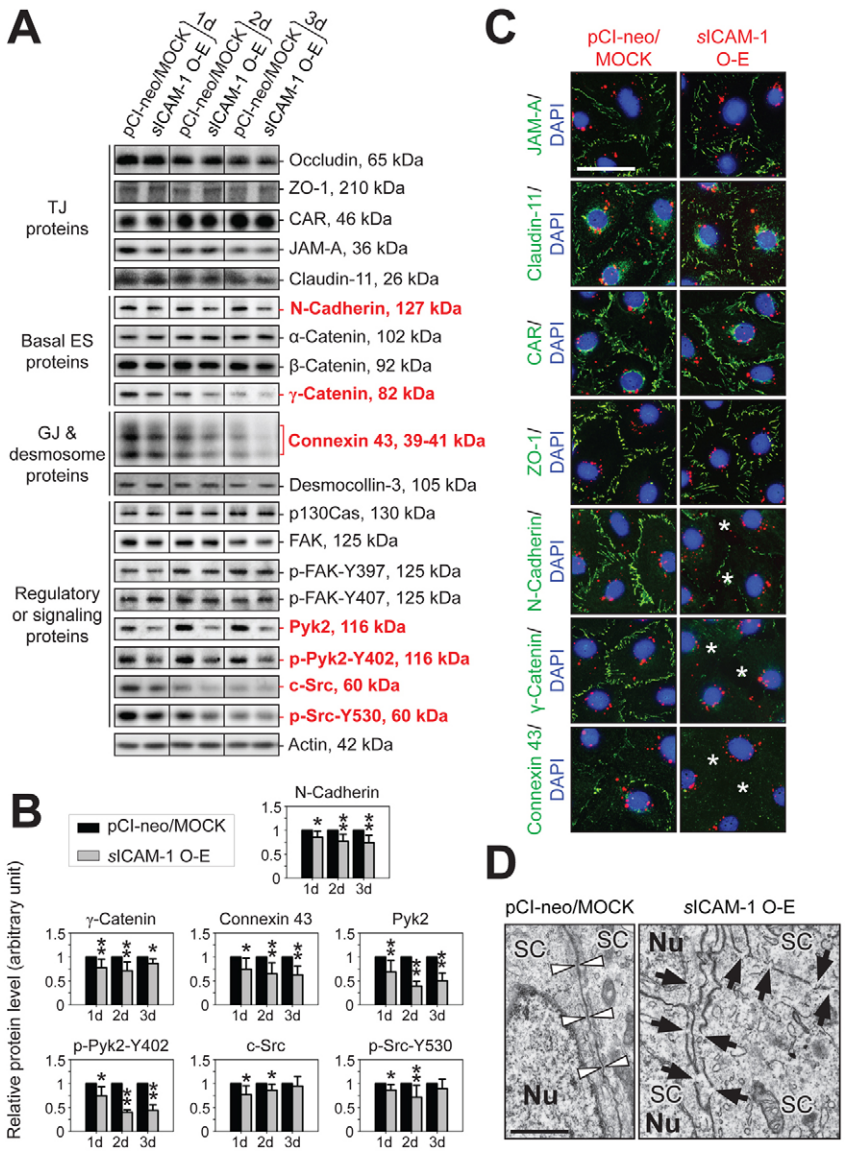

Fig. 5. Down-regulation of basal ES and GJ proteins at the Sertoli cell barrier by *s*ICAM-1 overexpression is mediated by Pyk2 and c-Src tyrosine kinases *in vitro*. (**A**) Sertoli cells were cultured for 2 days to establish a functional barrier. They were then transfected with pCI-neo/MOCK- or *s*ICAM-1-containing plasmids (see legend to Fig. 4 for additional details). Sertoli cells were terminated 1, 2 and 3 days (d) after transfection, and lysates were obtained for immunoblotting (supplementary material Table S2). Actin served as an internal control. Proteins whose steady-state levels changed following *s*ICAM-1 overexpression (O-E) versus pCI-neo/MOCK overexpression are labeled in red to the right of each immunoblot. Proteins are categorized as TJ, basal ES, GJ/desmosome and regulatory/signaling proteins to the left of the immunoblots. (**B**) Histograms summarizing immunoblotting results. Histograms are not shown for proteins whose steady-state levels did not change. Each data point was normalized against its corresponding actin data point, and then each *s*ICAM-1 overexpression data point was normalized against its corresponding pCI-neo/MOCK overexpression data point. pCI-neo/MOCK data points were arbitrarily set at 1. Each data point is a mean±s.d. of at least three independent experiments. Within a single experiment, each data point consisted of triplicate wells. (*$P<0.05$; **$P<0.01$). (**C**) Immunofluorescent staining of Sertoli cells 2 days after DNA transfection. Transfection efficiency was monitored by using Cy3^{TM}-labelled plasmid DNA (red). Sertoli cells were fixed with methanol and immunostained with antibodies against BTB constituent proteins (supplementary material Table S2). No changes were observed in JAM-A, claudin-11, CAR and ZO-1 (green) localization following *s*ICAM-1 overexpression. Asterisks denote changes in N-cadherin, γ-catenin and connexin 43 (green) localization following *s*ICAM-1 overexpression when compared with the corresponding controls. Cell nuclei were stained with DAPI (blue). Corresponding images were merged. Scale bar (applies to all panels)=50 μm. (**D**) Ultrastructural analysis by electron microscopy was performed on Sertoli cells 2 days after transfection with pCI-neo/MOCK- (left) or *s*ICAM-1- (right) containing plasmids. White arrowheads (left) point to an intact Sertoli cell barrier following pCI-neo/MOCK overexpression. Black arrows (right) point to a disrupted Sertoli cell barrier following *s*ICAM-1 overexpression. Scale bar (applies to both panels)=825 nm. Nu, nucleus; SC, Sertoli cell.

presented as a ratio of the two measurements (Fig. 6I). The diffusion of inulin-FITC into the adluminal compartment in testes from rats that received *s*ICAM-1-containing plasmids demonstrates BTB disruption (Fig. 6H,I). Ultrastructural analysis by electron microscopy also showed *s*ICAM-1 overexpression to disrupt the BTB *in vivo* (Fig. 6J).

*s*ICAM-1 overexpression *in vivo* down-regulates integral membrane proteins and disturbs F-actin integrity at the BTB

Since *s*ICAM-1 overexpression *in vitro* decreased the steady-state levels of N-cadherin and γ-catenin (Fig. 5), we decided to expand part of these results to the *in vivo* level (Fig. 7). Immunoblotting revealed no changes in the steady-state levels of occludin, CAR, desmoglein-2 and desmocollin-3 (Fig. 7A), consistent with *in vitro* data (Fig. 5). However, *s*ICAM-1 overexpression *in vivo* brought about a decrease in the levels of N-cadherin and connexin 43 (Fig. 7A,B). Following *s*ICAM-1 overexpression *in vivo*, no changes in occludin localization at the BTB were observed when compared with testes that were transfected with the pCI-neo/MOCK plasmid (Fig. 7Ce–h versus Fig. 7a–d). On the contrary, N-cadherin staining at the BTB became thinner and discontinuous (Fig. 7Cm–p versus Fig. 7i–l). Immunofluorescent staining of F-actin, a critical scaffolding protein, was also performed. In control testes, F-actin localized to the BTB and apical ES (Fig. 7Da–c) as previously described (Kopera et al., 2009; Sarkar et al., 2008). Following sICAM-1 overexpression, a loss of F-actin was observed at the BTB (Fig. 7Dd–f), illustrating BTB disruption. No changes in F-actin localization were noted at the site of the apical ES (Fig. 7Dd,e). Paraffin-embedded testes from overexpression experiments were also immunostained for desmoglein-2 (Fig. 7E). In control testes, desmoglein-2 localized largely to spermatocytes and early spermatids (Fig. 7Ea,a_1). However, no obvious changes in desmoglein-2 localization were noted following sICAM-1 overexpression (Fig. 7Ec,c_1,c_2). No staining was observed when anti-desmoglein-2 IgG was replaced with rabbit IgG (Fig. 7Eb). Finally, we summarize some of the findings reported in this study in a schematic illustration, which depicts the role of ICAM-1 and *s*ICAM-1 at the BTB (Fig. 7F).

Discussion

Herein, we report on the role of ICAM-1 in the mammalian testis. ICAM-1 is an Ig-like, membrane-bound adhesion molecule

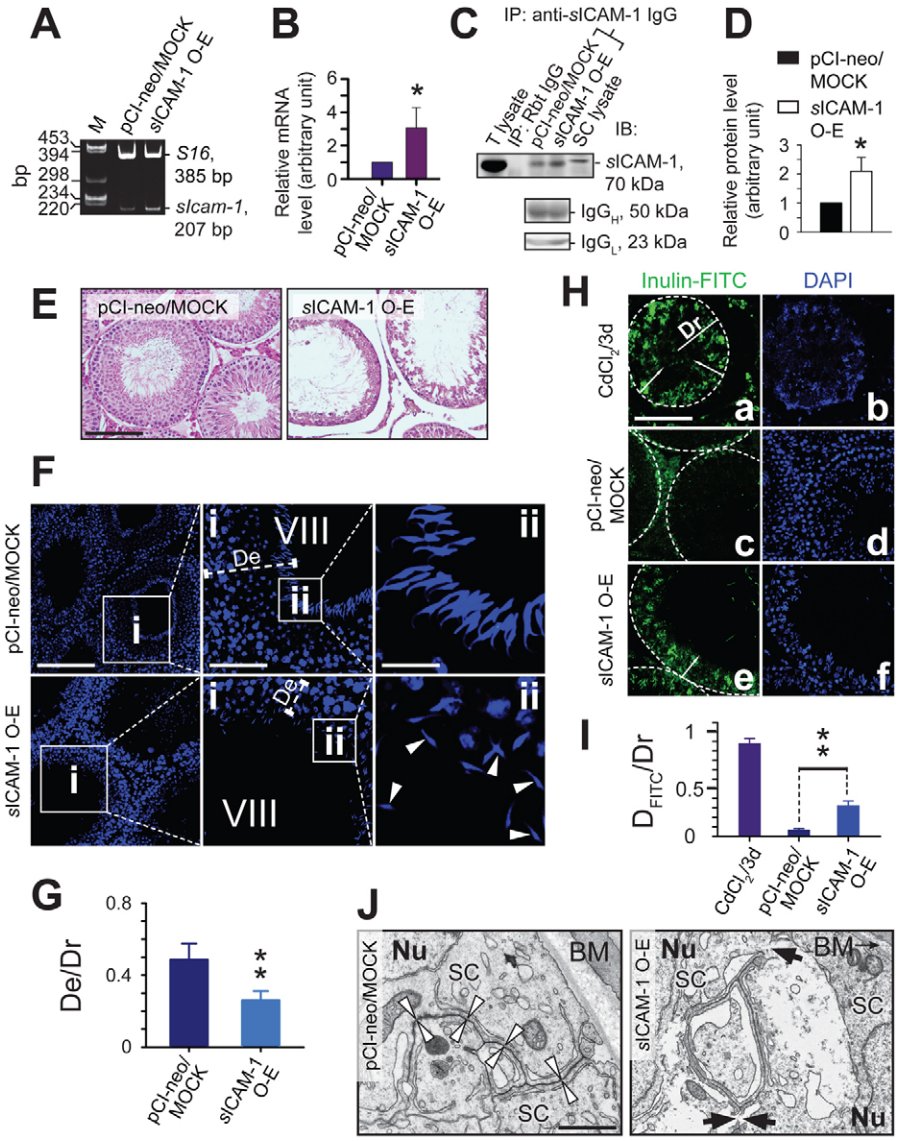

Fig. 6. See next page for legend.

Fig. 6. Analysis of spermatogenesis, germ cell adhesion and BTB integrity following *s*ICAM-1 overexpression. Semi-quantitative (**A**) and real-time (**B**) PCR results for *sIcam-1* using RNAs from testes 2 days after the last administration of pCI-neo/MOCK- or *s*ICAM-1-containing plasmids. For semi-quantitative PCR, a primer pair targeting an extracellular sequence of *Icam-1* was used to assess the efficiency of *s*ICAM-1 overexpression (O-E) (A) (supplementary material Table S1). *S16* (A) and *Gapdh* (B) were used as internal controls. bp, base pairs; M, DNA Molecular Weight Marker VI (Roche). The *sIcam-1* overexpression data was normalized against *Gapdh*, and then this value was normalized against its corresponding pCI-neo/MOCK overexpression data point (B). The pCI-neo/MOCK data point was arbitrarily set at 1. Each data point is a mean±s.d. of triplicate samples within a representative PCR experiment, and this experiment was repeated three times using cDNAs from different testes transfected with pCI-neo/MOCK- or *s*ICAM-1-containing plasmids (*$P<0.05$). It is worth noting that semi-quantitative and quantitative PCR experiments cannot reliably discriminate between *Icam-1* and *sIcam-1* expression, even if a primer pair targeting an extracellular sequence of ICAM-1 is used to amplify *s*ICAM-1. Although we have labeled PCR experiments as such for the sake of clarity, the inclusion of these data is only meant to support the results shown in (**C** and **D**). (C) Co-IP experiments were performed by using lysates from testes 2 days after the last administration of pCI-neo/MOCK- or *s*ICAM-1-containing plasmids. For the positive controls, testis (T, ~100 μg protein) and Sertoli cell (SC, ~60 μg protein) lysates were used without co-IP. For the negative control, anti-*s*ICAM-1 IgG was replaced with rabbit (Rbt) IgG (supplementary material Table S2). IgG_H and IgG_L represent IgG heavy and light chains, respectively. These representative immunoblots also show the uniform processing of samples. IB, immunoblotting; IP, immunoprecipitation. (D) Histogram summarizing co-IP/immunoblotting results. The *s*ICAM-1 overexpression data point was normalized against its corresponding pCI-neo/MOCK overexpression data point, which was arbitrarily set at 1. Each data point is a mean±s.d. of at least three independent co-IP experiments (*$P<0.05$). (**E**) Paraffin-embedded testes from rats 2 days after the last administration of pCI-neo/MOCK- or *s*ICAM-1-containing plasmids were cut at 5 μm, and sections were stained with hematoxylin and eosin. Scale bar (applies to both panels)=280 μm. (**F**) Frozen testes from rats 2 days after the last administration of pCI-neo/MOCK- or *s*ICAM-1-containing plasmids were cut at 7 μm, and sections were stained with DAPI (blue). Middle panels are magnified images of boxed areas in left panels, and right panels are magnified images of boxed areas in middle panels. Stages of the seminiferous epithelial cycle are denoted as roman numerals (top- and bottom-middle panels). White arrowheads (bottom-right panel) point to mis-oriented spermatids; scale bar, top left panel (also applies to bottom left panel)=200 μm; scale bar, top middle panel (also applies to bottom middle panel)=80 μm; scale bar, right panel (also applies to bottom right panel)=20 μm. De, seminiferous epithelium width. (**G**) Histogram summarizing morphometric analysis from overexpression experiments. Results are expressed as a ratio of the width of the seminiferous epithelium (De) to the radius of the seminiferous tubule (Dr). Each data point is a mean±s.d. of ~100 seminiferous tubules from each of 3–5 different rats, and at least ~300 tubules per treatment group were used in this analysis (**$P<0.01$). (**H**) To assess BTB function following *s*ICAM-1 overexpression, the diffusion of inulin-FITC (green) into the seminiferous epithelium from the systemic circulation was monitored by an integrity assay and fluorescence microscopy. For the positive control, rats received $CdCl_2$ (3 mg/kg b.w., i.p.), and they were used for BTB integrity assays 3 days after the administration of $CdCl_2$ (a,b). Testes from rats 2 days after the last administration of pCI-neo/MOCK- or sICAM-1-containing plasmids (c–f). Dashed curved lines (a,c,e) mark the periphery of seminiferous tubules. Arrows note the entry of (or lack thereof in the case of pCI-neo/MOCK) inulin-FITC into the adluminal compartment of the seminiferous epithelium. Cell nuclei were stained with DAPI. Scale bar in a (also applies to b–f)=130 μm. (**I**) Histogram summarizing morphometric analysis from BTB integrity experiments. Results are expressed as a ratio of the diffusion of inulin-FITC (D_{FITC}) to Dr. Each data point is a mean±s.d. of ~100 seminiferous tubules from each of 3–5 different rats, and at least ~300 tubules per treatment group were used in this analysis (**$P<0.01$). (**J**) Ultrastructural analysis by electron microscopy was performed on testes 2 days after the last administration of pCI-neo/MOCK- or *s*ICAM-1-containing plasmids. White arrowheads (left) point to an intact BTB following pCI-neo/MOCK overexpression. Large black arrows (right) point to a disrupted BTB following *s*ICAM-1 overexpression. Scale bar in left panel (also applies to right panel)=880 nm. BM, basement membrane; Nu, nucleus; SC, Sertoli cell.

expressed by several cell types, including Sertoli and germ cells in the testis (De Cesaris et al., 1998; Wong et al., 2000), and it is well known to function in the transendothelial migration of leukocytes (Lawson and Wolf, 2009; Long, 2011; Mamdouh et al., 2009; Muller, 2011). Immunolocalization studies showed ICAM-1 to be present at the site of the BTB, where its level was highest at stage VIII of the seminiferous epithelial cycle, coinciding with two critical cellular events that occur at this stage: the movement of preleptotene/leptotene spermatocytes across the BTB and the release of elongated spermatids into the tubule lumen (de Kretser and Kerr, 1988; Mruk and Cheng, 2004; Russell, 1993b). Weaker ICAM-1 immunoreactivity was also observed throughout the remaining seminiferous epithelium, as well as with elongating/elongated spermatids, and these observations are in line with ICAM's proposed roles in cell adhesion and cell migration (Lawson and Wolf, 2009; Long, 2011; Muller, 2011). Additional immunolocalization studies showed ICAM-1 to partially co-localize with BTB constituent proteins such as occludin, ZO-1, N-cadherin and β-catenin. Together with results obtained from co-IP experiments, which illustrated ICAM-1 to structurally associate with occludin-ZO-1 and N-cadherin-β-catenin protein complexes, we conclude that ICAM-1 is an integral component of the BTB where it probably contributes to barrier integrity. Indeed, ICAM-1 overexpression in Sertoli cells *in vitro* was found to enhance TJ permeability barrier function. These findings are intriguing for several reasons. First, they support the premise that BTB function is not constituted by TJs alone (in contrast to most other blood–tissue barriers) but by co-existing and co-functioning TJs, basal ESs, GJs and desmosomes where ICAM-1 plays a structural and/or signaling role. Second, they indicate that ICAM-1 may upregulate barrier function via cross-talk with occludin-ZO-1 and N-cadherin-β-catenin protein complexes. In addition, ICAM-1 was also found to associate with actin, suggesting that ICAM-1 may be involved in the remodeling of the Sertoli cell cytoskeleton, which is crucial for BTB integrity during preleptotene/leptotene spermatocyte movement. While ICAM-$1^{-/-}$ mice were viable, relatively healthy (for instance, their immune responses were impaired) and fertile (Sligh et al., 1993; Xu et al., 1994), an in-depth examination of BTB function in these animals is lacking. It is possible that BTB integrity is disrupted in a small percentage of seminiferous tubules such as those at stages VIII–XI but that mice remain fertile. In conclusion, it is possible that ICAM-1 is functioning to 'seal' the BTB during the movement of germ cells, somewhat similar to what occurs during the passage of leukocytes across the endothelium, but additional studies would need to be performed to substantiate this hypothesis.

While ICAM-1 is known to function in cell adhesion, significantly less is known about the role of *s*ICAM-1. *s*ICAM-1, which is derived from the proteolytic cleavage of membrane-bound ICAM-1, has been suggested in some biological contexts to have a role that is opposite to that of ICAM-1 (Clark et al., 2007). Interestingly, Sertoli cell barrier/BTB function was found to be compromised *in vitro* and *in vivo* following *s*ICAM-1 overexpression, illustrating that *s*ICAM-1 can negatively regulate

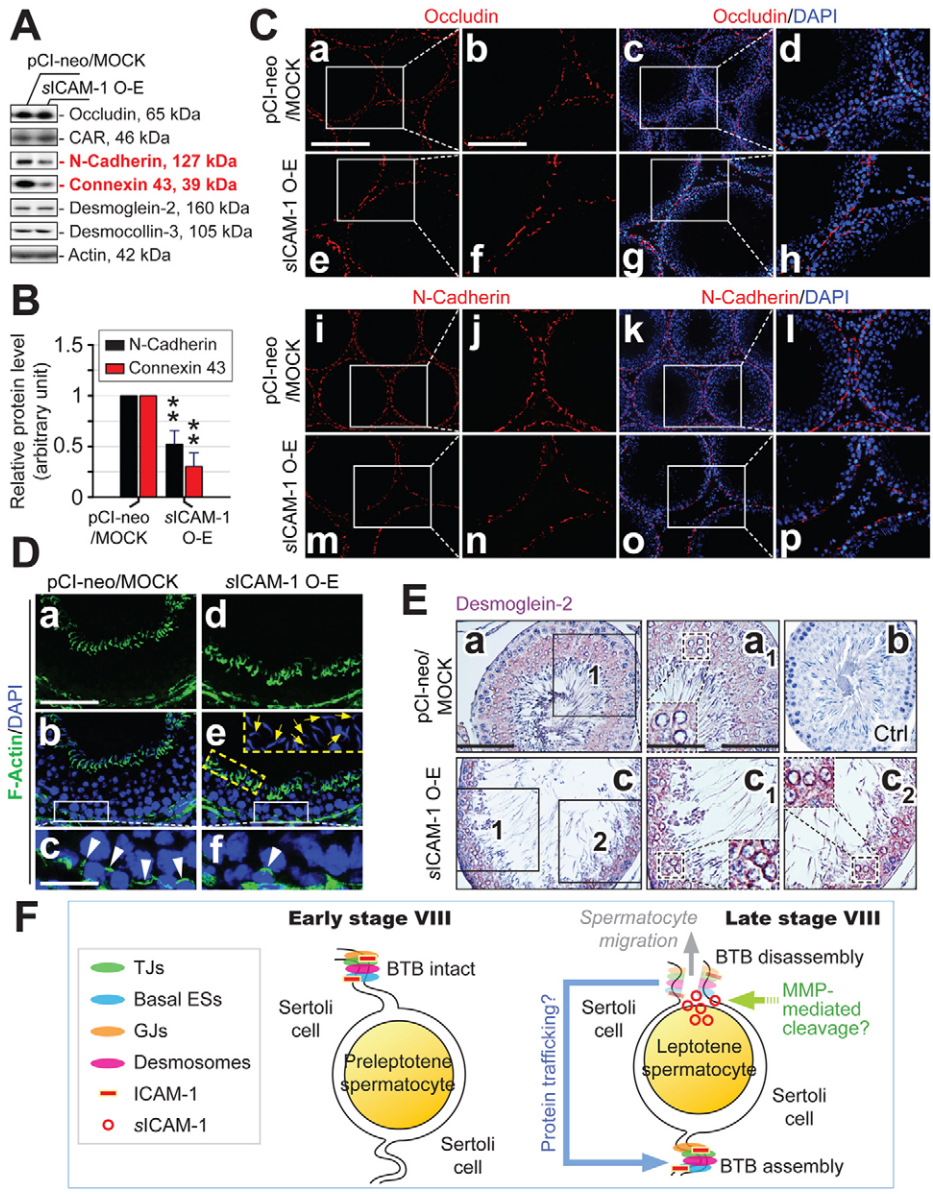

Fig. 7. Changes in the localization and steady-state levels of BTB constituent proteins following *s*ICAM-1 overexpression. (**A**) *s*ICAM-1 overexpression (O-E) decreases the steady-state levels of basal ES and GJ (but not TJ or desmosome) proteins in the testis. Proteins whose steady-state levels changed following *s*ICAM-1 overexpression versus pCI-neo/MOCK overexpression are labeled in red to the right of each immunoblot. Actin served as an internal control. (**B**) Histogram summarizing immunoblotting results. Histograms are not shown for proteins whose steady-state levels did not change. Each data point was normalized against its corresponding actin data point, and then each *s*ICAM-1 overexpression data point was normalized against its corresponding pCI-neo/MOCK overexpression data point. pCI-neo/MOCK data points were arbitrarily set at 1. Each data point is a mean±s.d. of triplicate samples within a representative experiment, and this experiment was repeated at least three times using different testes transfected with pCI-neo/MOCK- or *s*ICAM-1-containing plasmids. (**$P<0.01$). (**C**) Testes from rats 2–3 days after the last administration of pCI-neo/MOCK- or sICAM-1-containing plasmids were used for immunofluorescent staining (supplementary material Table S2). Boxed areas (a,c,e,g,i,k,m,o) correspond to magnified images (b,d,f,h,j,l,n,p), which better depict changes in protein localization. No changes were observed in occludin (red) localization following *s*ICAM-1 overexpression when compared with the pCI-neo/MOCK control (e–h versus a–d). However, a decrease in N-cadherin (red) localization was observed when compared with the corresponding control (m–p versus i–l). Cell nuclei were stained with DAPI (blue). Scale bar in a (also applies to c,e,g,i,k,m,o)=260 µm; scale bar in (b) (also applies to d,f,h,j,l,n,p)=130 µm. (**D**) Changes in F-actin (green) localization at the BTB after *s*ICAM-1 overexpression (d–f) versus pCI-neo/MOCK overexpression (a–c). Solid white line- and dashed yellow line-boxed areas (b,e) correspond to magnified images, which better depict changes in protein localization and changes in the relative orientation of spermatids. White arrowheads (f versus c) point to the loss of F-actin at the BTB. Yellow arrows point to the mis-orientation of spermatids. Scale bar in a (also applies to b,d,e)=90 µm; scale bar in c (also applies to f)=30 µm. (**E**) Paraffin-embedded testes from rats 2 days after the last administration of pCI-neo/MOCK- or *s*ICAM-1-containing plasmids were cut at 5 µm, and immunohistochemistry was performed using a desmoglein-2 antibody (supplementary material Table S2). For the control (Ctrl), anti-desmoglein-2 IgG was replaced with rabbit IgG, which was used at the same dilution (b). Boxed areas (a,a_1,c,c_1,c_2) correspond to magnified images, which better depict desmoglein-2 staining. Cell nuclei were stained with hematoxylin. Scale bar in a (also applies to b,c)=120 µm; scale bar in a_1 (also applies to c_1,c_2)=80 µm; scale bar in inset in a_1 (also applies to insets in c_1,c_2)=40 µm. (**F**) Schematic illustration summarizing our working hypothesis (see Discussion for additional details).

barrier function. This transient disruption in barrier dynamics was mediated by changes in the steady-state levels of basal ES (N-cadherin, γ-catenin) and GJ (connexin 43) proteins, which are known to be critical for BTB function, as well as by changes in tyrosine kinases (Pyk2/p-Pyk2-Y402 and c-Src/p-Src-Y530). For instance, a previous study showed the Sertoli cell TJ permeability barrier to be disrupted following downregulation of connexin 43 and plakophilin-2 (a desmosomal plaque protein that associates with connexin 43) (Li et al., 2009), demonstrating that GJs are critical for BTB function. ICAM-1 is also hypothesized to be regulated by Src and Pyk2. Src and Pyk2 are known to bind each other and to orchestrate the cascade of signaling events leading to cell movement (Gelman, 2003), suggesting that Src-Pyk2 may also be important in germ cell movement in the testis. Moreover, administration of PP1, a c-Src inhibitor, resulted in the loss of spermatocytes and round spermatids (but not elongating/elongated spermatids) from the seminiferous epithelium (Lee and Cheng, 2005). These results are similar to our findings following *s*ICAM-1 overexpression *in vivo* when germ cell sloughing was noted. Taken collectively, our data illustrate that *s*ICAM-1 may disrupt basal ESs and GJs situated above preleptotene/leptotene spermatocytes, resulting in Sertoli cell cytoskeleton remodeling, BTB disassembly and germ cell movement (Fig. 7F). In the testis, proteolytic cleavage of membrane-bound ICAM-1 may be mediated by matrix metalloprotease-9 (MMP-9), similar to reports in other epithelia and endothelia (Grenier and Bodet, 2008), resulting in the release of *s*ICAM-1 and in the timely disruption of BTB disassembly. This cleavage may be triggered by cytokines such as transforming growth factor-β (TGF-β), tumor necrosis factor α and interleukin-1α (IL-1α) or *s*ICAM-1 may be working with cytokines to regulate BTB dynamics because cytokines have been shown to disrupt barrier function (Lie et al., 2011; Lui et al., 2001; Lui et al., 2003). Indeed, ICAM-1 is known to be upregulated by pro-inflammatory cytokines (Inoue et al., 2011; Turner et al., 2011; Wertheimer et al., 1992). Another pool of *s*ICAM-1, produced by alternative splicing (Wakatsuki et al., 1995), may also exist in the seminiferous epithelium, and this pool may be interfering with ICAM-1-mediated cell adhesion above preleptotene/leptotene spermatocytes (Fig. 7F). While additional studies are needed, our results provide a framework upon which new experiments can be designed with the aim of better understanding the biology of the testis.

Materials and Methods

Animals and isolation of seminiferous tubules and germ cells

A female New Zealand white rabbit (3 kg b.w.) and male Sprague-Dawley rats at 90 (300 g b.w.) and 20 days-of-age were purchased from Charles River Laboratories (Kingston, NY). The use of animals was approved by The Rockefeller University Laboratory Animal Use and Care Committee (Protocol Numbers 09-016 and 12-506), and all experiments were conducted in accordance with ethical guidelines. Seminiferous tubules and total germ cells were isolated from testes of adult rats as previously described (Aravindan et al., 1996; Zwain and Cheng, 1994).

Isolation and culture of Sertoli cells

Sertoli cells were isolated from testes of 20-day-old rats and cultured in DMEM/F12 (Sigma-Aldrich, St Louis, MO) supplemented with growth factors and an antibiotic (Cheng et al., 1986; Mruk et al., 2003). Cells were seeded at a density of 0.5×10^6 cells/cm^2 in 12-well plates for lysate preparation, RNA isolation and overexpression experiments, at a density of 1.2×10^6 cells/cm^2 in Millicell inserts (Millipore Corp., Billerica, MA) for transepithelial electrical resistance (TER) measurements and overexpression experiments, or at a density of 0.05×10^6 cells/cm^2 on round glass coverslips (18 mm; Thomas Scientific, Swedesboro, NJ) for immunofluorescent staining. It is worth noting that functional junctions were assembled and maintained in control Sertoli cells cultured at all densities used in this study, a conclusion that is based on nearly two decades of research from this and other laboratories (Chung and Cheng, 2001; Chung et al., 1999; Dym and Papadopoulos, 1992; Florin et al., 2005; Hadley et al., 1987; Janecki et al., 1991; Janecki and Steinberger, 1986; Lie et al., 2011; Lui et al., 2001; Siu et al., 2003; Su et al., 2010b; Tung and Fritz, 1993). All substrata were coated with Matrigel™ basement membrane matrix as previously described (Xiao et al., 2011). Cultures were treated with a hypotonic buffer 36 hr after plating cells to remove contaminating germ cells (Galdieri et al., 1981), thereby yielding Sertoli cells with a purity of ~98% (Lee et al., 2004). Sertoli cell viability was assessed in random cultures throughout the entire study by using the Cell Proliferation kit (Roche, Indianapolis, IN).

Semi-quantitative and quantitative real-time RT–PCR

Total RNA from tissues and cells was obtained by using TRIzol® reagent (Invitrogen, Eugene, OR). Genomic DNA was removed from all samples by using deoxyribonuclease I (amplification grade, Invitrogen), and this was followed by an RT reaction. *S16* was incorporated into all semi-quantitative PCR experiments as an internal control (Xiao et al., 2011). For quantitative real-time PCR (qPCR), cDNAs were mixed with a SYBR® Green PCR master mix (Applied Biosystems Inc. [ABI], Foster City, CA), and the reaction was carried out by using an ABI 7900HT Fast Real-Time PCR system (Genomic Resource Center, The Rockefeller University). Data were analyzed by ABI SDS 2.3 software. The fold-change in mRNA was calculated according to the comparative C_T method ($2^{-\Delta\Delta C}{}_T$ method), and each data point was normalized against *Gapdh*. Supplementary material Table S1 lists the primer pairs and conditions that were used for all PCR experiments reported in this study.

Co-IP and immunoblotting

Co-IP and immunoblotting were performed as previously described (Xiao et al., 2011). Approximately 600–800 μg of total protein derived from testis, seminiferous tubule or Sertoli cell lysate was incubated with 2 (commercially available) or 15 μg (produced by us) anti-ICAM-1 or anti-*s*ICAM-1 IgG, respectively, followed by immunoblotting. Images were captured by using a Fujifilm LAS-4000 mini imaging system and analyzed in Multi Gauge software (version 3.1; Fujifilm, Valhalla, NY). Saturated images were not included in final statistical analyses. Each antibody was pre-screened in preliminary immunoblotting experiments by using lysates obtained from different testes to ensure that each antibody cross-reacted with its corresponding antigen of expected molecular weight. Also, in order to prevent overloading of gels with protein, which may have inadvertently obscured important changes in protein levels, preliminary immunoblotting experiments were used to pinpoint the quantity of lysate to be used for the detection of each antigen. In general, tissue lysates (including seminiferous tubule lysates) were used at 50–100 μg/lane, and cell lysates were used at 15–25 μg/lane, unless stated otherwise. Supplementary material Table S2 lists the antibodies and conditions that were used for all of the co-IP and immunoblotting experiments reported in this study. With regard to ICAM-1 and *s*ICAM antibodies, this table also clearly designates which antibody was used for each experiment.

Immunohistochemistry and immunofluorescent staining

Immunohistochemistry and immunofluorescent staining were performed as previously described by using the Histostain-Plus detection kit or reagents from Molecular Probes®/Invitrogen (Eugene, OR) with minor modifications to routine laboratory protocols (Xiao et al., 2011). Images were captured by using either a color (DS-Fi1-U2) or a monochromatic (Ds-Qi1Mc-U2) camera attached to a Nikon 90i motorized microscope and NIS-Elements AR software (version 3.2; Nikon Instruments Inc., Melville, NY). Images were compiled in Adobe Photoshop CS3 Extended software (version 10.0.1; Adobe Systems, San Jose, CA). If needed, color and fluorescent images were lightly modified for brightness and/or contrast, and all images within a single experimental group were modified using identical parameters. Supplementary material Table S2 lists the antibodies and conditions that were used for all of the immunohistochemistry and immunofluorescent staining experiments reported in this study.

Confocal and electron microscopy

Confocal microscopy was performed as previously described (Lie et al., 2011) by using Sertoli cells seeded at a density of ~$0.75–1.0\times10^6$ cells/cm^2 on Matrigel™-coated Transwell® permeable supports (24 mm; Corning, Lowell, MA). These cells were used for immunofluorescent staining as described above. Images were captured by using an inverted LSM 510 laser scanning confocal microscope and LSM 510 META software (Carl Zeiss, Thornwood, NY). Three-dimensional images were processed with ImageJ software (version 1.46, NIH), and the Richardson-Lucy deconvolution algorithm was used to reduce blur and/or noise associating with acquired images (Lucy, 1974; Richardson, 1972). Electron microscopy was performed as previously described (Lee and Cheng, 2003; Wong et al., 2004). Confocal and electron microscopy were performed at the

Bio-Imaging and Electron Microscopy Resource Centers, respectively, The Rockefeller University.

Production of recombinant *s*ICAM-1 and a polyclonal antibody against *s*ICAM-1

Primer pairs were prepared as previously described (Beck-Schimmer et al., 1998) (supplementary material Table S1), and a cDNA encoding domains 2 and 3 of rat extracellular ICAM-1 was generated by PCR using AccuPrime™ *Taq* DNA Polymerase High Fidelity (Invitrogen). Based on results presented herein (supplementary material Fig. S1), ICAM-2 is the only other ICAM known to be expressed by the testis so that a homology search was performed. When the amino acid sequence corresponding to domains 2 and 3 of ICAM-1 was compared against the entire ICAM-2 sequence, a ~38% similarity was noted, thereby illustrating minimal homology between proteins and little likelihood that the *s*ICAM-1 antibody would cross-react with ICAM-2. Thereafter, this cDNA was cloned into the pET-46 Ek/LIC vector and expressed in *Escherichia coli* BL21 (DE3) cells (EMD Chemicals, Gibbstown, NJ). The authenticity of the insert was verified by Sanger DNA sequencing (Genewiz, South Plainfield, NJ). Expression was induced with 0.4 mM isopropyl β-D-1-thiogalactopyranoside (IPTG) for 3 hr, and the production of His_6-tagged recombinant *s*ICAM-1 was verified first by a His_6 antibody (Roche, Indianapolis, IN) and second by an ICAM-1 antibody (Santa Cruz Biotechnology, Santa Cruz, CA) (supplementary material Table S2). It should be noted that this commercially available ICAM-1 antibody was raised against the extracellular domain of rat ICAM-1. Inclusion bodies were extracted from the insoluble cell fraction by using a BugBuster™ Plus Lysonase™ kit (EMD Chemicals), and the final pellet containing purified inclusion bodies was resuspended in guanidine lysis buffer (0.1 M NaH_2PO_4 pH 8.5 at 22℃ containing 10 mM Tris-HCl and 6 M guanidine HCl). The insoluble fraction extract was then purified by Ni ion affinity chromatography by using Ni Sepharose™ High Performance support (GE Healthcare) under denaturing conditions (0.1 M NaH_2PO_4 pH 8.0 at 22℃ containing 10 mM Tris-HCl and 8 M urea). Recombinant *s*ICAM-1 was stored in denaturing elution buffer (0.1 M NaH_2PO_4 pH 8.0 at 22℃ containing 10 mM Tris-HCl, 8 M urea and 200 mM imidazole), and its purity was assessed by Coomassie Blue staining. For antibody production, gel slices containing ~200 µg recombinant *s*ICAM-1 were equilibrated extensively against PBS (10 mM NaH_2PO_4 pH 7.4 at 22℃ containing 0.15 M NaCl). Gel slices were then sonicated/emulsified in Freund's complete adjuvant in a final volume of ~600 µl, and this was administered subcutaneously to the back of a New Zealand female rabbit at three different sites with ~200 µl being delivered per site. Three weeks thereafter the rabbit received a booster injection as described above, except that gel slices were sonicated/emulsified in Freund's incomplete adjuvant. The rabbit received yet another booster injection 3 weeks thereafter. Ten days thereafter blood was collected to obtain antiserum (Cheng and Bardin, 1987; Cheng et al., 1988b; Yan and Cheng, 2006), and IgG was isolated by $(NH_4)_2SO_4$ precipitation and DEAE-chromatography by using Macro-Prep® DEAE support (Bio-Rad Laboratories, Hercules, CA) (Cheng et al., 1988a; Page and Thorpe, 2001a; Page and Thorpe, 2001b).

Construction of ICAM-1, *s*ICAM-1 and ICAM-2 plasmids for subsequent overexpression

Rat full-length ICAM-1, *s*ICAM-1 and ICAM-2 cDNAs were amplified by PCR using AccuPrime™ *Taq* DNA Polymerase High Fidelity (Invitrogen) and corresponding primer pairs (supplementary material Table S1). For ICAM-1/*s*ICAM-1 overexpression plasmids, *Xho*I and *Mlu*I restriction sites were introduced into sense and antisense primers, respectively. On the other hand, *s*ICAM-1 was generated by a single nonsense mutation ($G^{1511}\rightarrow A^{1511}$) within the ICAM-1 transmembrane domain (Kita et al., 1992), resulting in a stop codon (TGG→TAG). For the ICAM-2 overexpression plasmid, *Mlu*I and *Xba*I restriction sites were introduced into sense and antisense primers, respectively. PCR products were cloned into the pCI-neo mammalian expression vector (Promega, Madison, WI). Thereafter, resulting plasmids were transformed into NovaBlue Singles™ Competent Cells (EMD Chemicals), purified by using a HiSpeed® plasmid Midi kit (Qiagen, Valencia, CA) and sequenced to verify authenticity (GENEWIZ).

Transient overexpression of ICAM-1, *s*ICAM-1 and ICAM-2 in Sertoli cells

Sertoli cells were isolated and cultured as described above. On day 2, cells were transfected with empty pCI-neo vector (MOCK, control), ICAM-1, *s*ICAM-1 or ICAM-2 plasmids using Effectene® transfection reagent (Qiagen). It should be noted that by this time *in vitro*, Sertoli cells had formed a polarized epithelium with functional TJs, basal ESs, desmosomes and GJs (Lee and Cheng, 2003; Lie et al., 2009; Siu et al., 2005; Wong et al., 2000), thereby mimicking the BTB *in vivo* (Byers et al., 1986; Chung et al., 2001; Chung et al., 1999; Siu et al., 2005; Steinberger and Jakubowiak, 1993; Yan et al., 2008). Thus, this excellent *in vitro* model has been, and continues to be, used by many investigators to study BTB dynamics. Pilot experiments were conducted to titrate the optimal quantity of DNA to be used for each application, and a 30-fold concentration range was tested (~0.1–3 µg) for each plasmid. Approximately 1 µg and 0.3 µg DNA was used for Sertoli cells cultured in 12-well plates and Millicell inserts, respectively. On the following day, media were replaced (this time point was designated as day 1 after transfection), after which cells were harvested daily for three consecutive days in lysis buffer (10 mM Tris pH 7.4 at 22℃ containing 0.15 M NaCl, 1% NP-40 [v/v] and 10% glycerol [v/v]; protease and phosphatase inhibitors were added at a 1:100 dilution immediately before use) or TRIzol® reagent (Invitrogen). For immunofluorescent staining of Sertoli cells, plasmid DNA was labeled by using the *Label* IT® Tracker™ intracellular nucleic acid localization kit (Mirus Bio, Madison, WI) at a 0.5:1 (v:w) ratio of Tracker™ reagent (Cy3™) to DNA to monitor transfection efficiency, and ~0.1 µg DNA was used for each transfection.

In vivo overexpression of *s*ICAM-1 in adult rat testes

Contamination of plasmid preparations by bacterial endotoxins was removed by using the MiraCLEAN® endotoxin removal kit (Mirus Bio). In brief, adult rats (~300 g b.w., $n=3$–5) received one intratesticular injection of a transfection mixture each day for three consecutive days. Each intratesticular injection consisted of 10 µg *s*ICAM-1 plasmid DNA in 200 µl *Trans*IT-EE Hydrodynamic Delivery Solution (Mirus Bio) administered via a 28-$G^1/_2$ insulin syringe so that the total amount of DNA that was injected and uptaken by cells in the testis, including Sertoli and germ cells, was 30 µg. The control consisted of administering the same amount of empty pCI-neo vector (MOCK). In this experiment, only the left testis was injected with plasmid DNA, whereas the right testis was left untreated. Rats were sacrificed 2 and 3 days after the last intratesticular injection, and testes were removed for subsequent analysis. Pilot experiments established the optimal quantity of DNA to be used, as well as the time of animal sacrifice.

BTB integrity assays

Adult rats (~300 g b.w., $n=3$–5) received one intratesticular injection of a transfection mixture each day for three consecutive days as previously described. Two days after the last administration of pCI-neo/MOCK- or *s*ICAM-1-containing plasmids, rats received ~1.5 mg inulin-FITC (Sigma-Aldrich) suspended in 300 µl PBS via the jugular vein under ketamine-HCl (60 mg/kg b.w.) and xylazine-HCl (15 mg/kg b.w.) anesthesia/analgesia as previously described (Kopera et al., 2009; Sarkar et al., 2008). Approximately 30 min thereafter, rats were euthanized by CO_2 asphyxiation, and testes were removed and snap-frozen in liquid nitrogen. Cryosections (relative thickness, 10 µm) were obtained, mounted with ProLong® Gold antifade reagent containing DAPI (4′,6-diamidino-2-phenylindole) (Invitrogen) and examined by fluorescent optics. The positive control consisted of treating rats ($n=2$) with $CdCl_2$ [3 mg/kg body weight (b.w.), intraperitoneally (i.p.)] and using these animals for BTB integrity assays 3 days after the administration of $CdCl_2$. $CdCl_2$ was used as a positive control because its disruptive effects on BTB function have been described in previously published reports (Elkin et al., 2010; Wong et al., 2004).

General methods

Total protein concentration was determined by using the D_C protein assay kit (Bio-Rad Laboratories) and a microplate reader (model 680, Bio-Rad Laboratories) with BSA as a standard. Quantitative protein data was obtained by using Scion Image (version 4.0.3.2; Scion Corporation, Houston, TX). Hematoxylin and eosin staining of paraffin-embedded testes was performed by a routine laboratory protocol. Sertoli cell barrier function was assessed daily with a Millicell electrical resistance system (Millipore Corp.) as previously described (Chung and Cheng, 2001). TER measurements consisted of passing short pulses (~2–3 sec) of current (20 µA) through the Sertoli cell epithelium using Ag/AgCl electrodes at 12, 3, 6 and 9 o'clock positions of the Millicell insert which were then averaged. Readings obtained from Matrigel™-coated 'blank' Millicell inserts (ones that did not contain any Sertoli cells) were then subtracted from each averaged value and subsequently multiplied by the effective growth surface area (0.6 cm^2). F-actin was stained as previously described (Kopera et al., 2009; Mruk and Lau, 2009; Sarkar et al., 2008).

Statistical analyses

Comparisons between two experimental groups were performed by Student's *t*-test, whereas comparisons among multiple experimental groups were performed by one-way ANOVA, followed by Dunnett's test. GB-STAT software (version 7.0; Dynamic Microsystems, Silver Spring, MD) was used for all statistical analyses. Each *in vitro* experiment was repeated 3–5 times using different batches of Sertoli cells. Within each *in vitro* experiment, each treatment point consisted of Sertoli cells cultured in 12-well plates, Millipore inserts or on glass coverslips in triplicate, unless stated otherwise. All *in vivo* experiments consisted of $n=3$–5 rats for each treatment point, except for rats that received $CdCl_2$ where $n=2$. $P<0.05$ was taken as statistically significant.

Acknowledgements

We thank Dr Kunihiro Uryu at the Electron Microscopy Resource Center, The Rockefeller University, for his excellent assistance in electron microscopy.

Funding

This work was supported in part by the National Institute of Child Health and Human Development, the National Institutes of Health

[grant numbers R03 HD061401 to D.D.M., R01 HD056034 and U54 HD029990 Project 5 to C.Y.C.]. Deposited in PMC for release after 12 months.

Supplementary material available online at
http://jcs.biologists.org/lookup/suppl/doi:10.1242/jcs.107987/-/DC1

References

Aravindan, G. R., Pineau, C. P., Bardin, C. W. and Cheng, C. Y. (1996). Ability of trypsin in mimicking germ cell factors that affect Sertoli cell secretory function. *J. Cell. Physiol.* **168**, 123-133.

Beck-Schimmer, B., Schimmer, R. C., Schmal, H., Flory, C. M., Friedl, H. P., Pasch, T. and Ward, P. A. (1998). Characterization of rat lung ICAM-1. *Inflamm. Res.* **47**, 308-315.

Byers, S. W., Hadley, M. A., Djakiew, D. and Dym, M. (1986). Growth and characterization of polarized monolayers of epididymal epithelial cells and Sertoli cells in dual environment culture chambers. *J. Androl.* **7**, 59-68.

Cheng, C. Y. and Bardin, C. W. (1987). Identification of two testosterone-responsive testicular proteins in Sertoli cell-enriched culture medium whose secretion is suppressed by cells of the intact seminiferous tubule. *J. Biol. Chem.* **262**, 12768-12779.

Cheng, C. Y. and Mruk, D. D. (2002). Cell junction dynamics in the testis: Sertoli-germ cell interactions and male contraceptive development. *Physiol. Rev.* **82**, 825-874.

Cheng, C. Y. and Mruk, D. D. (2009). An intracellular trafficking pathway in the seminiferous epithelium regulating spermatogenesis: a biochemical and molecular perspective. *Crit. Rev. Biochem. Mol. Biol.* **44**, 245-263.

Cheng, C. Y. and Mruk, D. D. (2012). The blood-testis barrier and its implications for male contraception. *Pharmacol. Rev.* **64**, 16-64.

Cheng, C. Y., Mather, J. P., Byer, A. L. and Bardin, C. W. (1986). Identification of hormonally responsive proteins in primary Sertoli cell culture medium by anion-exchange high performance liquid chromatography. *Endocrinology* **118**, 480-488.

Cheng, C. Y., Mathur, P. P. and Grima, J. (1988a). Structural analysis of clusterin and its subunits in ram rete testis fluid. *Biochemistry* **27**, 4079-4088.

Cheng, C. Y., Chen, C. L., Feng, Z. M., Marshall, A. and Bardin, C. W. (1988b). Rat clusterin isolated from primary Sertoli cell-enriched culture medium is sulfated glycoprotein-2 (SGP-2). *Biochem. Biophys. Res. Commun.* **155**, 398-404.

Chung, N. P. Y. and Cheng, C. Y. (2001). Is cadmium chloride-induced inter-Sertoli tight junction permeability barrier disruption a suitable in vitro model to study the events of junction disassembly during spermatogenesis in the rat testis? *Endocrinology* **142**, 1878-1888.

Chung, S. S., Lee, W. M. and Cheng, C. Y. (1999). Study on the formation of specialized inter-Sertoli cell junctions in vitro. *J. Cell. Physiol.* **181**, 258-272.

Chung, N. P. Y., Mruk, D. D., Mo, M. Y., Lee, W. M. and Cheng, C. Y. (2001). A 22-amino acid synthetic peptide corresponding to the second extracellular loop of rat occludin perturbs the blood-testis barrier and disrupts spermatogenesis reversibly in vivo. *Biol. Reprod.* **65**, 1340-1351.

Clark, P. R., Manes, T. D., Pober, J. S. and Kluger, M. S. (2007). Increased ICAM-1 expression causes endothelial cell leakiness, cytoskeletal reorganization and junctional alterations. *J. Invest. Dermatol.* **127**, 762-774.

Cyr, D. G., Hermo, L., Egenberger, N., Mertineit, C., Trasler, J. M. and Laird, D. W. (1999). Cellular immunolocalization of occludin during embryonic and postnatal development of the mouse testis and epididymis. *Endocrinology* **140**, 3815-3825.

De Cesaris, P., Starace, D., Riccioli, A., Padula, F., Filippini, A. and Ziparo, E. (1998). Tumor necrosis factor-α induces interleukin-6 production and integrin ligand expression by distinct transduction pathways. *J. Biol. Chem.* **273**, 7566-7571.

de Kretser, D. M. and Kerr, J. B. (1988). The cytology of the testis. In *The Physiology of Reproduction* (ed. E. Knobil, J. B. Neill, L. L. Ewing, G. S. Greenwald, C. L. Markert and D. W. Pfaff), pp. 837-932. New York, NY: Raven Press.

Durieu-Trautmann, O., Chaverot, N., Cazaubon, S., Strosberg, A. D. and Couraud, P. O. (1994). Intercellular adhesion molecule 1 activation induces tyrosine phosphorylation of the cytoskeleton-associated protein cortactin in brain microvessel endothelial cells. *J. Biol. Chem.* **269**, 12536-12540.

Dustin, M. L., Rothlein, R., Bhan, A. K., Dinarello, C. A. and Springer, T. A. (1986). Induction by IL 1 and interferon-γ: tissue distribution, biochemistry, and function of a natural adherence molecule (ICAM-1). *J. Immunol.* **137**, 245-254.

Dym, M. and Papadopoulos, V. (1992). Dual compartment (bicameral) culture: role of basement membrane in epithelial differentiation. *Cell Biol. Toxicol.* **8**, 55-59.

Elkin, N. D., Piner, J. A. and Sharpe, R. M. (2010). Toxicant-induced leakage of germ cell-specific proteins from seminiferous tubules in the rat: relationship to blood-testis barrier integrity and prospects for biomonitoring. *Toxicol. Sci.* **117**, 439-448.

Florin, A., Maire, M., Bozec, A., Hellani, A., Chater, S., Bars, R., Chuzel, F. and Benahmed, M. (2005). Androgens and postmeiotic germ cells regulate claudin-11 expression in rat Sertoli cells. *Endocrinology* **146**, 1532-1540.

Galdieri, M., Ziparo, E., Palombi, F., Russo, M. A. and Stefanini, M. (1981). Pure Sertoli cell cultures: a new model for the study of somatic-germ cell interactions. *J. Androl.* **5**, 249-259.

Gearing, A. J., Hemingway, I., Pigott, R., Hughes, J., Rees, A. J. and Cashman, S. J. (1992). Soluble forms of vascular adhesion molecules, E-selectin, ICAM-1, and VCAM-1: pathological significance. *Ann. N. Y. Acad. Sci.* **667**, 324-331.

Gelman, I. H. (2003). Pyk 2 FAKs, any two FAKs. *Cell Biol. Int.* **27**, 507-510.

Grenier, D. and Bodet, C. (2008). *Streptococcus suis* stimulates ICAM-1 shedding from microvascular endothelial cells. *FEMS Immunol. Med. Microbiol.* **54**, 271-276.

Hadley, M. A., Djakiew, D., Byers, S. W. and Dym, M. (1987). Polarized secretion of androgen-binding protein and transferrin by Sertoli cells grown in a bicameral culture system. *Endocrinology* **120**, 1097-1103.

Hellani, A., Ji, J. W., Mauduit, C., Deschildre, C., Tabone, E. and Benahmed, M. (2000). Developmental and hormonal regulation of the expression of oligodendrocyte-specific protein/claudin 11 in mouse testis. *Endocrinology* **141**, 3012-3019.

Inoue, T., Kobayashi, K., Inoguchi, T., Sonoda, N., Fujii, M., Maeda, Y., Fujimura, Y., Miura, D., Hirano, K. and Takayanagi, R. (2011). Reduced expression of adipose triglyceride lipase enhances tumor necrosis factor α-induced intercellular adhesion molecule-1 expression in human aortic endothelial cells via protein kinase C-dependent activation of nuclear factor-κB. *J. Biol. Chem.* **286**, 32045-32053.

Janecki, A. and Steinberger, A. (1986). Polarized Sertoli cell functions in a new two-compartment culture system. *J. Androl.* **7**, 69-71.

Janecki, A., Jakubowiak, A. and Steinberger, A. (1991). Regulation of transepithelial electrical resistance in two-compartment Sertoli cell cultures: in vitro model of the blood-testis barrier. *Endocrinology* **129**, 1489-1496.

Kita, Y., Takashi, T., Iigo, Y., Tamatani, T., Miyasaka, M. and Horiuchi, T. (1992). Sequence and expression of rat ICAM-1. *Biochim. Biophys. Acta* **1131**, 108-110.

Kopera, I. A., Su, L., Bilinska, B., Cheng, C. Y. and Mruk, D. D. (2009). An in vivo study on adjudin and blood-testis barrier dynamics. *Endocrinology* **150**, 4724-4733.

Lawson, C. and Wolf, S. (2009). ICAM-1 signaling in endothelial cells. *Pharmacol. Rep.* **61**, 22-32.

Lee, N. P. Y. and Cheng, C. Y. (2003). Regulation of Sertoli cell tight junction dynamics in the rat testis via the nitric oxide synthase/soluble guanylate cyclase/3′,5′-cyclic guanosine monophosphate/protein kinase G signaling pathway: an in vitro study. *Endocrinology* **144**, 3114-3129.

Lee, N. P. Y. and Cheng, C. Y. (2005). Protein kinases and adherens junction dynamics in the seminiferous epithelium of the rat testis. *J. Cell. Physiol.* **202**, 344-360.

Lee, N. P. Y., Mruk, D. D., Conway, A. M. and Cheng, C. Y. (2004). Zyxin, axin, and Wiskott-Aldrich syndrome protein are adaptors that link the cadherin/catenin protein complex to the cytoskeleton at adherens junctions in the seminiferous epithelium of the rat testis. *J. Androl.* **25**, 200-215.

Li, M. W. M., Mruk, D. D., Lee, W. M. and Cheng, C. Y. (2009). Connexin 43 and plakophilin-2 as a protein complex that regulates blood-testis barrier dynamics. *Proc. Natl. Acad. Sci. USA* **106**, 10213-10218.

Lie, P. P. Y., Cheng, C. Y. and Mruk, D. D. (2010). The desmoglein-2/desmocollin-2/Src kinase protein complex regulates blood-testis barrier dynamics. *Int. J. Biochem. Cell Biol.* **42**, 975-986.

Lie, P. P. Y., Cheng, C. Y. and Mruk, D. D. (2011). Interleukin-1α is a regulator of the blood-testis barrier. *FASEB J.* **25**, 1244-1253.

Long, E. O. (2011). ICAM-1: getting a grip on leukocyte adhesion. *J. Immunol.* **186**, 5021-5023.

Lucy, L. B. (1974). An iterative technique for the rectification of observed distributions. *Astron. J.* **79**, 745-754.

Lui, W. Y., Lee, W. M. and Cheng, C. Y. (2001). Transforming growth factor-β3 perturbs the inter-Sertoli tight junction permeability barrier in vitro possibly mediated via its effects on occludin, zonula occludens-1, and claudin-11. *Endocrinology* **142**, 1865-1877.

Lui, W. Y., Lee, W. M. and Cheng, C. Y. (2003). Transforming growth factor β3 regulates the dynamics of Sertoli cell tight junctions via the p38 mitogen-activated protein kinase pathway. *Biol. Reprod.* **68**, 1597-1612.

Mamdouh, Z., Mikhailov, A. and Muller, W. A. (2009). Transcellular migration of leukocytes is mediated by the endothelial lateral border recycling compartment. *J. Exp. Med.* **206**, 2795-2808.

Marlin, S. D., Staunton, D. E., Springer, T. A., Stratowa, C., Sommergruber, W. and Merluzzi, V. J. (1990). A soluble form of intercellular adhesion molecule-1 inhibits rhinovirus infection. *Nature* **344**, 70-72.

Millán, J., Hewlett, L., Glyn, M., Toomre, D., Clark, P. and Ridley, A. J. (2006). Lymphocyte transcellular migration occurs through recruitment of endothelial ICAM-1 to caveola- and F-actin-rich domains. *Nat. Cell Biol.* **8**, 113-123.

Mruk, D. D. and Cheng, C. Y. (2004). Sertoli-Sertoli and Sertoli-germ cell interactions and their significance in germ cell movement in the seminiferous epithelium during spermatogenesis. *Endocr. Rev.* **25**, 747-806.

Mruk, D. D. and Cheng, C. Y. (2008). Delivering non-hormonal contraceptives to men: advances and obstacles. *Trends Biotechnol.* **26**, 90-99.

Mruk, D. D. and Lau, A. S. N. (2009). RAB13 participates in ectoplasmic specialization dynamics in the rat testis. *Biol. Reprod.* **80**, 590-601.

Mruk, D. D., Siu, M. K. Y., Conway, A. M., Lee, N. P. Y., Lau, A. S. N. and Cheng, C. Y. (2003). Role of tissue inhibitor of metalloproteases-1 in junction dynamics in the testis. *J. Androl.* **24**, 510-523.

Muller, W. A. (2011). Mechanisms of leukocyte transendothelial migration. *Annu. Rev. Pathol.* **6**, 323-344.

Nourshargh, S., Hordijk, P. L. and Sixt, M. (2010). Breaching multiple barriers: leukocyte motility through venular walls and the interstitium. *Nat. Rev. Mol. Cell Biol.* **11**, 366-378.

O'Donnell, L., Nicholls, P. K., O'Bryan, M. K., McLachlan, R. I. and Stanton, P. G. (2011). Spermiation: The process of sperm release. *Spermatogenesis* **1**, 14-35.

Page, M. and Thorpe, R. (2001a). Purification of IgG by precipitation with sodium sulfate or ammonium sulfate. In *The Protein Protocols Handbook* (ed. J. M. Walker), pp. 983-984. Totowa, NJ: Humana Press.

Page, M. and Thorpe, R. (2001b). Purification of IgG using DEAE-Sepharose chromatography. In *The Protein Protocols Handbook* (ed. J. M. Walker), pp. 987-988. Totowa, NJ: Humana Press.

Prozialeck, W. C., Edwards, J. R. and Woods, J. M. (2006). The vascular endothelium as a target of cadmium toxicity. *Life Sci.* **79**, 1493-1506.

Riccioli, A., Filippini, A., De Cesaris, P., Barbacci, E., Stefanini, M., Starace, G. and Ziparo, E. (1995). Inflammatory mediators increase surface expression of integrin ligands, adhesion to lymphocytes, and secretion of interleukin 6 in mouse Sertoli cells. *Proc. Natl. Acad. Sci. USA* **92**, 5808-5812.

Richardson, W. H. (1972). Bayesian-based iterative method of image restoration. *JOSA* **62**, 55-59.

Rothlein, R., Dustin, M. L., Marlin, S. D. and Springer, T. A. (1986). A human intercellular adhesion molecule (ICAM-1) distinct from LFA-1. *J. Immunol.* **137**, 1270-1274.

Rothlein, R., Mainolfi, E. A., Czajkowski, M. and Marlin, S. D. (1991). A form of circulating ICAM-1 in human serum. *J. Immunol.* **147**, 3788-3793.

Russell, L. D. (1993a). Morphological and functional evidence for Sertoli-germ cell relationships. In *The Sertoli Cell* (ed. L. D. Russell and M. D. Griswold), pp. 365-390. Clearwater, FL: Cache River Press.

Russell, L. D. (1993b). Role in spermiation. In *The Sertoli Cell* (ed. L. D. Russell and M. D. Griswold), pp. 269-303. Clearwater, FL: Cache River Press.

Sarkar, O., Mathur, P. P., Cheng, C. Y. and Mruk, D. D. (2008). Interleukin 1 α (IL1A) is a novel regulator of the blood-testis barrier in the rat. *Biol. Reprod.* **78**, 445-454.

Siu, M. K. Y., Lee, W. M. and Cheng, C. Y. (2003). The interplay of collagen IV, tumor necrosis factor-α, gelatinase B (matrix metalloprotease-9), and tissue inhibitor of metalloproteases-1 in the basal lamina regulates Sertoli cell-tight junction dynamics in the rat testis. *Endocrinology* **144**, 371-387.

Siu, M. K., Wong, C. H., Lee, W. M. and Cheng, C. Y. (2005). Sertoli-germ cell anchoring junction dynamics in the testis are regulated by an interplay of lipid and protein kinases. *J. Biol. Chem.* **280**, 25029-25047.

Siu, E. R., Wong, E. W. P., Mruk, D. D., Sze, K. L., Porto, C. S. and Cheng, C. Y. (2009). An occludin-focal adhesion kinase protein complex at the blood-testis barrier: a study using the cadmium model. *Endocrinology* **150**, 3336-3344.

Sligh, J. E., Jr, Ballantyne, C. M., Rich, S. S., Hawkins, H. K., Smith, C. W., Bradley, A. and Beaudet, A. L. (1993). Inflammatory and immune responses are impaired in mice deficient in intercellular adhesion molecule 1. *Proc. Natl. Acad. Sci. USA* **90**, 8529-8533.

Steinberger, A. and Jakubowiak, A. (1993). Sertoli cell culture: historical perspective and review of methods. In *The Sertoli Cell* (ed. L. D. Russell and M. D. Griswold), pp. 155-180. Clearwater, FL: Cache River Press.

Stolpe, A. and Saag, P. T. (1996). Intercellular adhesion molecule-1. *J. Mol. Med.* **74**, 13-33.

Su, L., Cheng, C. Y. and Mruk, D. D. (2010a). Adjudin-mediated Sertoli-germ cell junction disassembly affects Sertoli cell barrier function in vitro and in vivo. *Int. J. Biochem. Cell Biol.* **42**, 1864-1875.

Su, L., Mruk, D. D., Lee, W. M. and Cheng, C. Y. (2010b). Differential effects of testosterone and TGF-β3 on endocytic vesicle-mediated protein trafficking events at the blood-testis barrier. *Exp. Cell Res.* **316**, 2945-2960.

Tung, P. S. and Fritz, I. B. (1993). Interactions of Sertoli cells with laminin are essential to maintain integrity of the cytoskeleton and barrier functions of cells in culture in the two-chambered assembly. *J. Cell. Physiol.* **156**, 1-11.

Turner, N. A., Das, A., O'Regan, D. J., Ball, S. G. and Porter, K. E. (2011). Human cardiac fibroblasts express ICAM-1, E-selectin and CXC chemokines in response to proinflammatory cytokine stimulation. *Int. J. Biochem. Cell Biol.* **43**, 1450-1458.

Wakatsuki, T., Kimura, K., Kimura, F., Shinomiya, N., Ohtsubo, M., Ishizawa, M. and Yamamoto, M. (1995). A distinct mRNA encoding a soluble form of ICAM-1 molecule expressed in human tissues. *Cell Adhes. Commun.* **3**, 283-292.

Wang, C. Q. F., Mruk, D. D., Lee, W. M. and Cheng, C. Y. (2007). Coxsackie and adenovirus receptor (CAR) is a product of Sertoli and germ cells in rat testes which is localized at the Sertoli-Sertoli and Sertoli-germ cell interface. *Exp. Cell Res.* **313**, 1373-1392.

Wertheimer, S. J., Myers, C. L., Wallace, R. W. and Parks, T. P. (1992). Intercellular adhesion molecule-1 gene expression in human endothelial cells. Differential regulation by tumor necrosis factor-α and phorbol myristate acetate. *J. Biol. Chem.* **267**, 12030-12035.

Witkowska, A. M. and Borawska, M. H. (2004). Soluble intercellular adhesion molecule-1 (sICAM-1): an overview. *Eur. Cytokine Netw.* **15**, 91-98.

Wong, C. C. S., Chung, S. S. W., Grima, J., Zhu, L. J., Mruk, D. D., Lee, W. M. and Cheng, C. Y. (2000). Changes in the expression of junctional and nonjunctional complex component genes when inter-Sertoli tight junctions are formed in vitro. *J. Androl.* **21**, 227-237.

Wong, C. H., Mruk, D. D., Lui, W. Y. and Cheng, C. Y. (2004). Regulation of blood-testis barrier dynamics: an in vivo study. *J. Cell Sci.* **117**, 783-798.

Xiao, X., Mruk, D. D., Lee, W. M. and Cheng, C. Y. (2011). c-Yes regulates cell adhesion at the blood-testis barrier and the apical ectoplasmic specialization in the seminiferous epithelium of rat testes. *Int. J. Biochem. Cell Biol.* **43**, 651-665.

Xu, H., Gonzalo, J. A., St Pierre, Y., Williams, I. R., Kupper, T. S., Cotran, R. S., Springer, T. A. and Gutierrez-Ramos, J. C. (1994). Leukocytosis and resistance to septic shock in intercellular adhesion molecule 1-deficient mice. *J. Exp. Med.* **180**, 95-109.

Yan, H. H. N. and Cheng, C. Y. (2006). Laminin α3 forms a complex with β3 and γ3 chains that serves as the ligand for α6β1-integrin at the apical ectoplasmic specialization in adult rat testes. *J. Biol. Chem.* **281**, 17286-17303.

Yan, H. H. N., Mruk, D. D., Lee, W. M. and Cheng, C. Y. (2008). Blood-testis barrier dynamics are regulated by testosterone and cytokines via their differential effects on the kinetics of protein endocytosis and recycling in Sertoli cells. *FASEB J.* **22**, 1945-1959.

Yang, L., Froio, R. M., Sciuto, T. E., Dvorak, A. M., Alon, R. and Luscinskas, F. W. (2005). ICAM-1 regulates neutrophil adhesion and transcellular migration of TNF-α-activated vascular endothelium under flow. *Blood* **106**, 584-592.

Zwain, I. H. and Cheng, C. Y. (1994). Rat seminiferous tubular culture medium contains a biological factor that inhibits Leydig cell steroidogenesis: its purification and mechanism of action. *Mol. Cell. Endocrinol.* **104**, 213-227.